Model-Based Measurement of Diffusion Using Raman Spectroscopy

André Bardow and Wolfgang Marquardt
Lehrstuhl für Prozesstechnik, RWTH Aachen, Turmstrasse 46, D-52064 Aachen, Germany

Volker Göke, Hans-Jürgen Koss, and Klaus Lucas
Lehrstuhl für Technische Thermodynamik, RWTH Aachen, Schinkelstrasse 8, D-52056 Aachen, Germany

The measurement of diffusion coefficients in multicomponent liquid mixtures is still an open question. A new technique aimed at overcoming this deficiency is presented. It is based on Raman spectroscopy, which has been extended to obtain liquid concentration data of all components in a mixture simultaneously with high temporal and spatial resolution. The following data analysis uses model-based methods. This provides a very flexible framework, allowing substantial reduction of experimental effort and time and the direct estimation of the diffusion coefficient as a function of concentration. Furthermore, the experimental procedure is improved using optimal experimental design techniques. This new methodology is validated for binary mixtures.

Introduction

Diffusion is the rate-limiting step in many mass-transfer operations, such as distillation, extraction, absorption, and in (heterogeneous) chemical reactions. Therefore, knowledge about the laws describing the diffusive mass transport is required in order to design mass-transfer equipment. In the case of nonideal liquid mixtures, the diffusion rate can only be calculated with large uncertainty (Reid et al., 1987). For multicomponent mixtures the model structure itself is not known (Taylor and Krishna, 1993). This is due to the limited amount of data available on multicomponent diffusion coefficients.

Today, there are a number of established methods for the measurement of constant diffusion coefficients in binary and ternary mixtures, for example, interferometry (Miller et al., 1993) and Taylor dispersion (Leaist, 1990). The equipment is specialized to diffusion measurements and the experiments last rather long. The main drawback of these methods is that they rely on scalar quantities like the refractive index or the conductivity, which cannot be associated unambiguously with concentration in the case of multicomponent systems. Therefore, measurements of diffusion in quaternary mixtures are already very scarce. To our knowledge quaternary diffusion coefficients in nonelectrolyte mixtures have only been measured in one case (Rai and Cullinan, 1973).

On the other hand, techniques based on spectroscopy do allow the direct determination of the mole fractions of all components in a mixture. Today, these concentration measurements are still expected to be less precise than those with established methods. But spectroscopic methods will allow faster measurements in multicomponent and even reactive mixtures. Therefore, we are developing a novel procedure for the measurement of diffusion in liquids using Raman spectroscopy.

In addition we use model-based techniques for the analysis and design of the experiments. In the established methods several assumptions have to be made in order to simplify the analysis. Furthermore, additional experimental effort is required in order to obtain a step profile as an initial condition. These restrictions do not apply to our approach. A detailed model of the process is used and arbitrary initial conditions can be handled. The model further allows the use of optimal experimental design techniques where the free variables of the experimental procedure are chosen in order to improve the precision in the measured diffusion coefficient. Finally, the model-based approach offers the possibility for an in-depth analysis of the experiments.

The measured Fick diffusion coefficients are in general a strong function of composition (Taylor and Krishna, 1993). This dependence is usually estimated from several point measurements of the diffusion coefficient that are then interpolated, usually by a low-order polynomial function. The se-

Correspondence concerning this article should be addressed to W. Marquardt.

lection of the number of experiments and of an adequate function for interpolation is usually not rigorously analyzed. In contrast, the method presented here allows the direct estimation of the concentration dependence of the diffusion coefficient.

In this article our methodology for binary diffusion as the natural starting point for a new measurement principle is presented. Experimental results are given for the system of toluene and cyclohexane to validate the new approach. The final aim of our research is the development of a flexible and fast model-based measurement procedure for studying mass transfer in multicomponent mixtures, even including reactions at a later point of time.

Experiment

In the last years, Raman spectroscopy has been extended to one-dimensional (Mewes et al., 1999; Rabenstein et al., 1998) and two-dimensional (Grünefeld et al., 2000; Kyritsis et al., 2000) noninvasive measurements of concentration in multicomponent mixtures. Depending on the application, the method has been optimized either toward spatial or temporal high-resolution or toward the precise determination of concentrations. In this work we have improved precision as well as spatial and temporal resolution at the same time. We are now able to observe the concentration profiles of both components in diffusive mass transfer with sufficient accuracy and resolution for the measurement of diffusion coefficients.

Experimental setup

The experimental setup for the measurement of diffusion by Raman spectroscopy is shown in Figure 1. It consists of four main parts and is mounted on an antivibration table.

The focused beam (50 μm) of an argon ion laser (Spectra Physics, excitation wavelength 514.5 nm, power 0.5 to 10 W) is directed through the diffusion cell filled with a liquid sample. We use a simple square quartz cell with inner dimensions of $10\times10\times40$ mm. The measuring line extends from the very bottom of the cell up to a height of 8 to 10 mm, always including the initial boundary zone. In transparent samples only a negligible amount of energy is absorbed by the liquid. Since varying the (low) stimulating laser power has no perceptible influence on the shape of concentration profiles local heating at the laser beam can be neglected.

A macrolens (Nikon Nikkor 200 mm 1:4D) collects the Raman signal at an angle of 90°. Afterwards the signal is cleared up by a holographic NOTCH filter (Kaiser Optics). Here we use a narrow bandwidth filter to eliminate the disturbing, much more intensive stimulating wavelength. Another lens focuses the signal toward the entrance slit of the spectrograph (ARC Spectra Pro 500 i).

The grating of the spectrograph—with 300 or 1200 lambert (L)/mm, depending on the required resolution—resolves the first-order diffraction into a spectrum without distorting the one-dimensional image of the measuring line. The two-dimensional image created this way (one spatial and one spectral dimension) is recorded by an air-cooled charge-coupled device camera (Roper Scientific NTE/CCD-1340/400). The photosensitive chip (back-illuminated) has an efficiency of about 90% (conversion from a photon to an electron) in the considered wavelength range of 500 to 600 nm. Every row of the chip, a total of 400, is collecting the Raman spectrum from a small segment of the one-dimensional measuring line. The dimension of this segment is called spatial resolution and at present measures 20 to 25 μm per row, depending on the particular system studied. After one exposure, the data col-

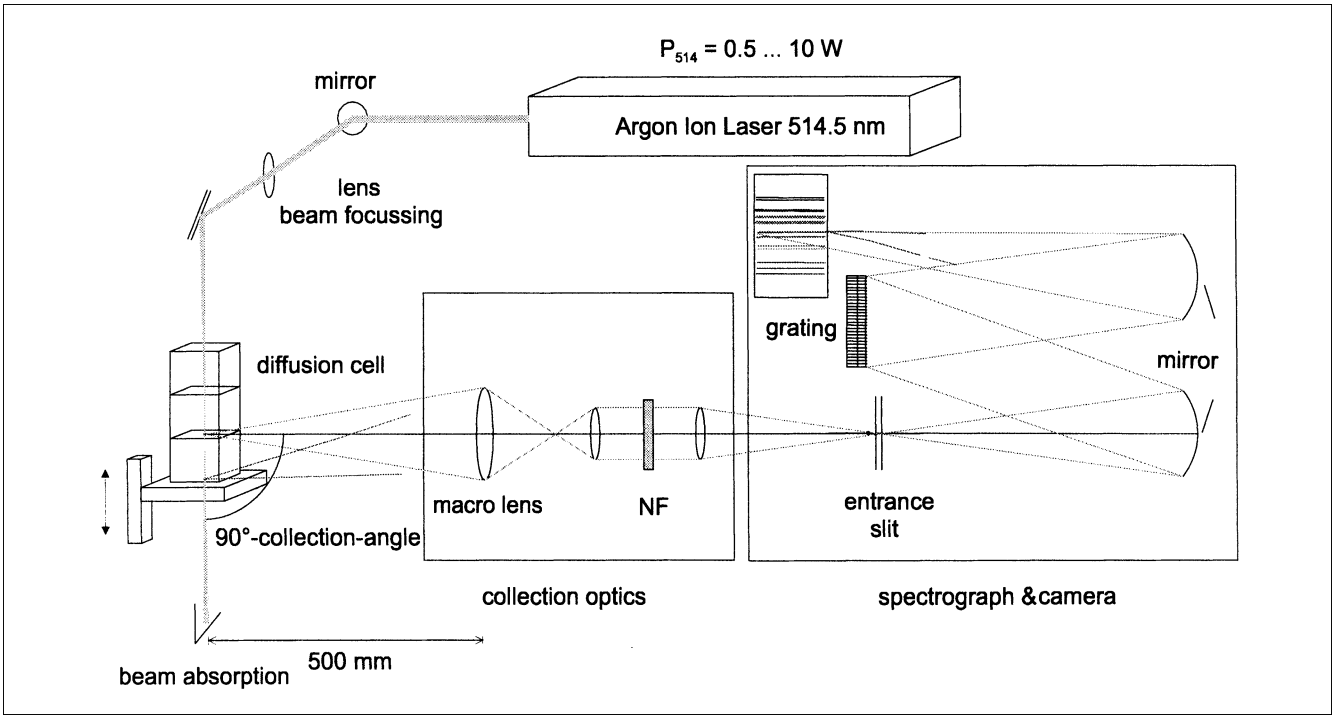

Figure 1. Experimental setup.

lected by the chip have to be stored. This leads to a minimal time delay for the next earliest possible exposure, which amounts from 10 s for full spatial resolution down to 1.5 s for reduced spatial resolution with only 50 instead of 400 data points.

The most complicated step in the preparation of a series of experiments is the adjustment of the entrance slit to the optical axis of the beam passing the diffusion cell. A precise alignment is possible, because the best position is related to the maximum signal intensity over the entire image height.

Spectra analysis and calibration

In this section a short overview about our procedure of Raman spectra analysis will be given. The spectra are used here to obtain the mole fractions of all components in a liquid mixture. A detailed presentation of the analysis of overlapping spectra can be found in Koss et al. (2001).

One of the basic assumptions of Raman spectroscopy and the basis of calibration is the existence of a linear relationship between the intensity of a signal and the concentration for each component. The measured intensity, I_i, at the frequency ν can then be expressed as

$$I_i(\nu)\Delta\tau = \frac{\Phi}{r^2\pi} c_i \frac{s_i}{c_i} d\Delta\tau\epsilon_O(\nu). \tag{1}$$

For a single exposure, the stimulating power, Φ, the radius of the laser beam, r, and the thickness of the irradiated sample $d = 2r$, the time $\Delta\tau$ of exposure, and the total optical efficiency ϵ_O are constant for all components, while the molar concentration, c_i, and the Raman scattering coefficient, s_i (Schrader, 1995), may differ. To reduce statistical errors, the spectrum is analyzed in an interval $[\nu_{\min}, \nu_{\max}]$, which contains all characteristic vibrational bands. Integrating over this frequency range leads to the so-called integrated intensity $A_i\ (\nu_{\min}, \nu_{\max})$

$$A_i(\nu_{\min}, \nu_{\max})\Delta\tau = \frac{\Phi}{r^2\pi} c_i d\Delta\tau \int_{\nu_{\min}}^{\nu_{\max}} \frac{s_i}{c_i}\epsilon_O(\nu). \tag{2}$$

In a mixture with n_c components, the species j is chosen as a reference component. Dividing (Eq. 2) by the intensity of the reference component, the expression becomes

$$\frac{A_i(\nu_{\min}, \nu_{\max})}{A_j(\nu_{\min}, \nu_{\max})} = \frac{c_i}{c_j} \frac{\int_{\nu_{\min}}^{\nu_{\max}} \frac{s_i}{c_i}\epsilon_O(\nu)d\nu}{\int_{\nu_{\min}}^{\nu_{\max}} \frac{s_j}{c_j}\epsilon_O(\nu)d\nu} = \frac{c_i}{c_j} k_{ij}(\nu_{\min}, \nu_{\max}), \tag{3}$$

where the proportionality factor $k_{ij}\ (\nu_{\min}, \nu_{\max})$ between the ratios of molar concentration and the integrated intensities has to be determined by calibration. Since the frequency interval, $[\nu_{\min}, \nu_{\max}]$, is the same for all measurements, the dependency of A_i and k_{ij} on it is omitted in the following.

Calibration

For a mixture of n_c components, at least $n_c - 1$ linear independent proportionality factors, k_{ij}, have to be determined. These factors may depend on the position and concentration due to systematic errors concerning the optical adjustment and further spectra analysis.

We calibrate our assembly in so-called spatially resolved mode: a one-dimensional Raman spectrum of a homogeneous sample is recorded. Instead of adding the signal of all array detector rows first and analyzing it afterwards, the spectrum of every single row z is analyzed individually. The parameter $k_{ij}(z)$ can be calculated from

$$k_{ij}(z) = \frac{A_i(z)/A_j(z)}{c_i(z)/c_j(z)}. \tag{4}$$

By division by the arithmetic mean value of k_{ij} (averaged over all 400 rows of the detector), a specific spatial correction is calculated. It is typically less than 1% of the average value. By this procedure it is possible to detect and correct local optical distortions.

Spectral analysis

In order to compute the proportionality factor from Eq. 4, the integrated intensities, A_i, have to be inferred from the spectral measurements. Recently, a new computational technique for spectra analysis has been developed by Koss et al. (2001), which is more flexible than, for example, PLS methods. In PLS methods nonlinearities have to be compensated by superposing the nonphysical Eigen values, whereby the number of parameters increases. In contrast to this statistical correction, we interpret, for example, a lateral movement of a Raman band as a physical property of the spectrum studied. More important is the fact that PLS methods fail in the analysis of reactive mixtures, where some components cannot be set in a known concentration in the calibration procedure. Our method does allow the interpretation of such systems. This will be important for future research activities of studying reactions and diffusion simultaneously. The developed method itself is a general-purpose tool applicable to other spectral methods.

A mathematical model of the spectrum has to be generated for every component of the mixture. Gauss, Lorentz, and Voigt profiles are used to approximate the spectrum. For each profile values of the position, the relative height and the half width at half maximum (HWHM) are calculated (Figure 2). Asymmetrical bands require an additional superposing of smaller profiles to minimize the difference between the measured spectrum and the mathematical models. This is, for example, necessary on both sides of the 802.5 cm^{-1} band of cyclohexane. The background is usually fitted by a horizontal straight line. For the optimization process the Levenberg–Marquardt algorithm is used.

In ideal systems the pure substance spectra strictly superpose in the mixture and just have to be arithmetically weighted within the fitting procedure. Spectra of thermodynamically nonideal mixtures differ slightly from direct superposing due to molecular interaction. These spectra can be analyzed if some free variables are introduced, allowing, for example, a lateral movement of one Raman band. Position, relative

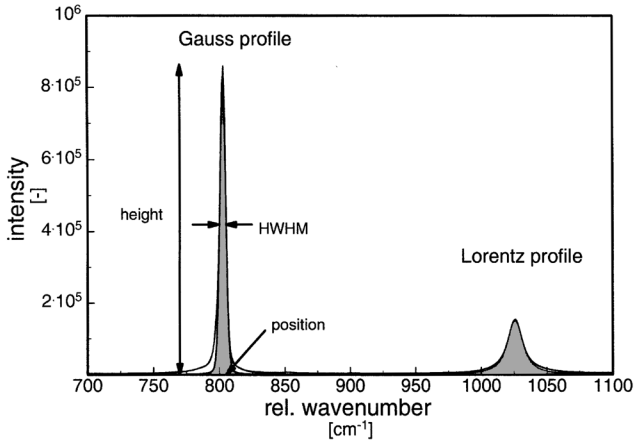

Figure 2. Principle of substance modeling: first approximation of two strong bands of cyclohexane.

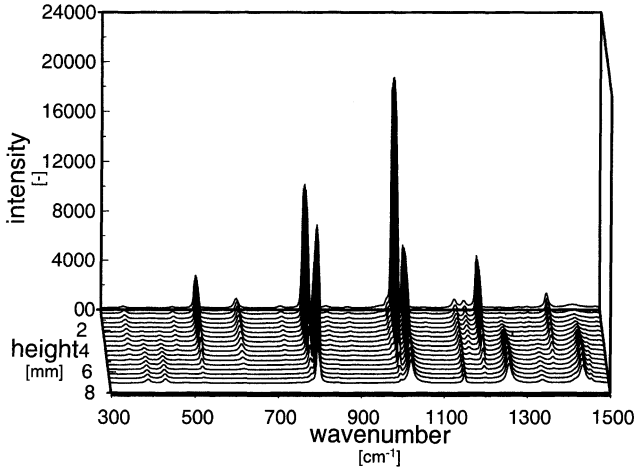

Figure 3. Shape of Raman spectra, depending on position.

height, and FWHM from pure substances are used as initial values.

By this procedure a mathematical model of the spectrum is obtained and the integrated intensities, A_i, can be computed. It should be noted that it is not necessary to assign the individual bands to particular vibrational modes of a molecule for our purpose.

In the calibration step these integrated intensities are measured for mixtures of known composition, and the proportionality constant is calculated using Eq. 4.

Estimation of concentrations

In order to measure the concentrations of each component in an unknown mixture, a spectrum model is developed as described earlier. The integrated intensities, A_i, of all components are evaluated. The mole fraction of each component in a mixture can then be calculated with the knowledge of the proportionality factor k_{ij} from

$$x_i = \frac{c_i/c_j}{\sum_{l=1}^{n_c} c_l/c_j} = \left(\sum_{l=1}^{n_c} \frac{c_l}{c_i} \right)^{-1} = \left(\sum_{l=1}^{n_c} \frac{A_l}{A_i} \frac{1}{k_{lj}} \right)^{-1}. \quad (5)$$

This procedure allows the estimation of the concentrations with a high accuracy. The absolute statistical error for the mole fractions $x_{i,\ \text{calc.}} - x_{i,\ \text{true value}}$ is less than 0.0015 (0.15 %), while the relative local systematic deviations are estimated to be smaller than 0.005 (0.5%). These error estimates were obtained by measurement of samples with known composition that were not used during calibration and from the diffusion experiments shown below.

Diffusion experiment

Before each series of experiments is started the adjustment of the assembly is checked. First it is necessary that the bottom of the diffusion cell is situated in the lower section of the measuring line. The magnification factor (MF), which relates the length of the measuring line in the diffusion cell to the corresponding image on the CCD detector, is obtained by recording a transparent ruled grating positioned in the measuring plane. The number of rows between two minima of intensity on the chip, resulting from the dark marks of the scale, are counted and averaged. In our experiments no spatial dependency was found within the accuracy of the array detector with discrete lines. This shows that the influence of a refractive-index gradient over the height of the cell on the magnification factor can be neglected. Finally, the spectra of several calibration samples are recorded. They are taken from pure substances (FLUKA, purity 99.8 mass percent, no further purification) and six to ten homogeneous mixtures. These solutions are prepared by mass. The calibration procedure is repeated after the experiment to check for optical distortion during the time of the main experiment.

We perform restricted diffusion experiments, where the concentrations at the bottom of the cell as well as the liquid–vapor interface change during time. This is in contrast to most other research groups using optical techniques to study diffusion (Miller et al., 1993). It is more complex to receive good optical quality of the signal near the bottom of the cell due to reflections of the laser beam at the quartz surface. But there is the advantage that the concentration profiles contain much more information about the diffusion model we want to determine (see below). We also use rather large concentration differences with $\Delta x_i \approx 0.2$ between the two initial phases. This is not a lower limit for the measurement technique, but it is our aim to reduce the number of experiments required to determine the concentration dependence of the diffusion coefficient. Besides, undesirable convective mixing, resulting from density inversion, is a minor problem in our approach.

The quartz cell is first filled with the lighter solution up to four-fifths of its inner height. Then, the denser solution is injected below carefully with the help of a syringe pump (ABG). The filling is stopped when the denser solution has reached a level of about 2–5 mm, measured from the bottom of the cell. Then, the cell is closed with a thin PTFE-greased glass cover. Now we take the first record, typically 120 s after the beginning of substrating. The interval between two pictures varies from 1 to 3 min, depending on the dynamics of

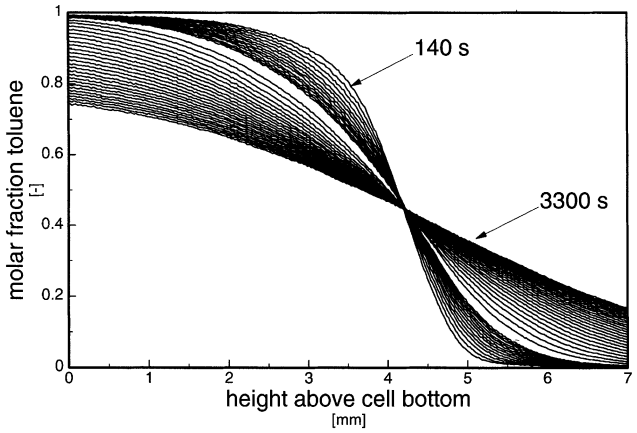

Figure 4. Time-dependent concentration profiles of toluene during a diffusion experiment.

the expected transport process, which is influenced by the initial concentration difference and the diffusion coefficient. Figure 3 illustrates the different shapes taken from an early record during the diffusion experiment of cyclohexane and toluene. Spectra in the back at low row numbers of the height coordinate result from the composition near the bottom of the cell and refer to nearly pure toluene. The actual diffusion zone is located in the region from 4 to 6 mm, where the spectra from both pure substances overlap. Raman spectra in the front of the figure—representing the top of cell—belong to pure cyclohexane.

The time-dependent concentration profiles of each component are calculated automatically (Figure 4) from the ratio of integral intensities (Eq. 3) and the calibration coefficient $k_{ij}(z)$. Obviously, the quality of the data with respect to noise is excellent; they are the basis for the estimation of the diffusion coefficient.

In the first series of experiments we recorded the temperature in the cell, but have not yet used a temperature-controlled cell. During a single experiment the change in temperature was always less than 0.2 K, which has a rather small influence on the speed of diffusion. We are currently building a temperature-controlled diffusion cell, so that we will not have to convert the measured data of different days with slightly differing temperatures (1 to 3 K) to a standard temperature anymore, where small errors can always occur.

Model Development

In order to employ model-based techniques for the analysis of the diffusion experiment, a model describing the process with sufficient accuracy is needed. In the established diffusion-measuring procedures it is usually assumed that the concentration difference between the two phases is small enough to assume a constant Fick diffusion coefficient and to neglect any volume effects (Cussler, 1976). The diffusion is regarded relative to the volume-average velocity, which is zero according to the stated assumptions. This leads to the model

$$\frac{\partial c_i}{\partial t} = D^V \frac{\partial^2 c_i}{\partial z^2}, \tag{6}$$

which can be solved analytically for different boundary conditions (Crank, 1975). This model allows the use of direct estimation schemes for the diffusion coefficient, but prevented the use of model-based experimental design techniques. In addition the experiments are conducted in diffusion cells with free diffusion boundary conditions in order to avoid experimental difficulties at the boundaries of the diffusion cell and to get a simpler analysis (Dunlop et al., 1972). The resulting value for the Fick diffusion coefficient in the volume-average reference frame has then to be converted to the molar-average reference frame in order to be compared with the models proposed from theory (see Taylor and Krishna, 1993, Chapt. 3, Sec. 3.2.4).

As stated earlier, we want to be able to cover larger concentration ranges in one experiment in order to estimate the Fick diffusion coefficient over the whole concentration range from just a few measurements. In addition, it seems beneficial to estimate the diffusion coefficients in the molar-average reference frame directly. A constant Fick diffusion coefficient in the molar reference frame allows a better description of the diffusion process for a wider concentration range, since the coefficient in the volume-average frame is a stronger function of composition. Furthermore, the new experimental technique is designed to analyze multicomponent mixtures. Therefore, we had to develop another model for the process. The model consists of the total mole balance

$$\frac{\partial c_t}{\partial t} + \frac{\partial}{\partial z}(c_t v_z^*) = 0, \tag{7}$$

the component balances

$$c_t\left(\frac{\partial x_i}{\partial t} + v_z^* \cdot \frac{\partial x_i}{\partial z}\right) = -\frac{\partial J_i}{\partial z}, \qquad i = 1, \ldots, n_c - 1, \tag{8}$$

and the closing condition

$$0 = 1 - \sum_{i=1}^{n_c} x_i. \tag{9}$$

This model needs to be supplemented by an equation of state. For many mixtures the volume of mixing can be neglected. The total molar concentration, c_t, can therefore be described by

$$\frac{1}{c_t} = \sum_{i=1}^{n_c} x_i V_{i0}(T), \tag{10}$$

assuming an ideal mixture. The model thus specified has a differential index of 2. Index reduction by differentiation (Unger et al., 1995) gives the following algebraic equation for the molar velocity:

$$v_z^* = -\sum_{i=1}^{n_c} J_i V_{i0}(T), \tag{11}$$

which corresponds to $u^V = 0$. This relation replaces the total mole balance (Eq. 7).

For mixtures not allowing the assumption of an ideal mixture (Eq. 10), the molar concentration can be described as

$$\frac{1}{c_t} = \sum_{i=1}^{n_c} x_i V_{i0}(T) + V^E(x_1, \ldots, x_{n_c}). \tag{12}$$

Then, the algebraic equation (Eq. 11) is replaced by

$$\frac{1}{c_t}\frac{\partial c_t v_z^*}{\partial z} = \sum_{i=1}^{n_c-1}\left[(V_{i0} - V_{n0}) + \left(\frac{\partial V^E}{\partial x_i} - \frac{\partial V^E}{\partial x_n}\right)\right] \times \left(-c_t v_z^* \cdot \frac{\partial x_i}{\partial z} - \frac{\partial J_i}{\partial z}\right), \tag{13}$$

with $v_z^*(t,0) = 0$. For mixtures with large excess volume effects the contraction of the total liquid volume has to be considered. The extension to this case is straightforward if a suitable coordinate transformation is used (see, e.g., Bausa and Marquardt, 2001).

Finally, a model has to be specified for the diffusive flux J_i. In order to compare our results to measurements from the literature, we used Fick's law

$$J_1 = -c_t D \frac{\partial x_1}{\partial z}. \tag{14}$$

In the case of binary diffusion, the Fick diffusion coefficient, D, can be directly related to the Maxwell–Stefan diffusion coefficient, $Đ$ (Taylor and Krishna, 1993) by

$$D = Đ \cdot \left(1 + x_1 \frac{\partial \ln \gamma_1}{\partial x_1}\right). \tag{15}$$

These models can be solved with standard software for dynamic simulation. In our work we use the commercial simulation environment gPROMS (gPROMS Technical Document, 2001).

Experimental Design

Experimental results can be substantially improved by employing model-based optimal experimental design techniques [for a survey, see Walter and Pronzato (1990)]. Therefore, we want to enhance our new experimental procedure using these methods. There are some applications in the area of heat transfer (Taktak et al., 1993; Alifanov, 1994; Emery and Nenarokomov, 1998), but to our knowledge this approach has not been applied to the analysis of mass-diffusion phenomena.

The goal of our analysis is the precise estimation of the diffusion coefficient, D, from the mole-fraction measurements, $x(t_j, z_k)$, available from Raman spectroscopy. The experiment can be described in an abstract way as

$$x(t_j, z_k) = f(t_j, z_k, D, x_0, \boldsymbol{p}), \qquad j = 1, \ldots, J; \quad k = 1, \ldots, K, \tag{16}$$

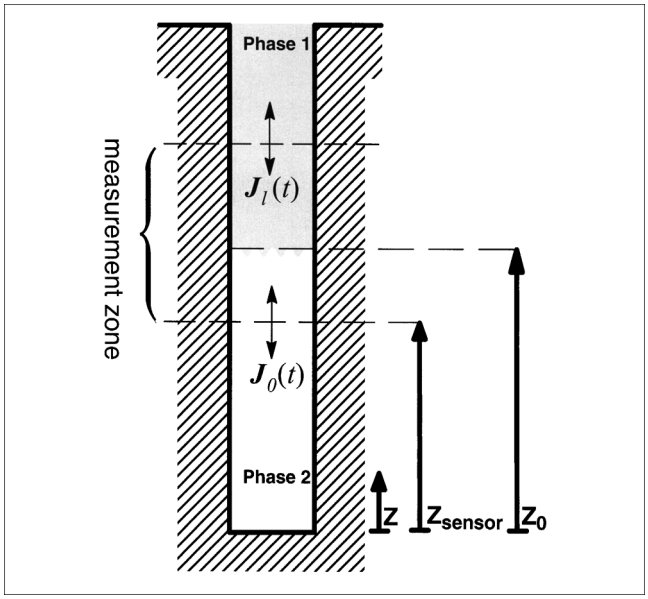

Figure 5. Diffusion cell.

where f represents the experiment itself, including the measuring procedure. This function depends on the unknown diffusion coefficient, D, the initial condition, x_0, and the parameter vector, $\boldsymbol{p}$, representing experimental settings. The experimental setup (Figure 5) leaves several design variables free to be chosen by the experimenter:

- The position of the measurement zone, $p_1 = z_{\text{sensor}}$
- The initial amount of the lower phase, $p_2 = z_0$
- The duration of the experiment, $p_3 = t_{\text{end}}$.

These parameters should be chosen so as to maximize the precision in the final estimate of the diffusion coefficient, D.

A measure for the precision of the estimate is its variance. An estimate for the variance can be given by the inverse of the Fisher information matrix, which reduces to a scalar in the case of one unknown considered here. It can be stated under common assumptions as (Walter and Pronzato, 1990)

$$F = \sum_{i=1}^{N} w_i \left(\frac{\partial x}{\partial D}\right)^2, \tag{17}$$

where w_i denotes the weight of measurement i in the estimation procedure. This weight is usually chosen as the inverse variance of the measurement error (Bard, 1974).

In recent years the techniques of optimal experimental design have been extended to include models of partial differential equations (e.g., Emery and Nenarokomov, 1998; Dieses et al., 2000; Vande Wouwer et al., 2000). All these investigations deal with one spatial dimension. The problem is reduced to an optimal control problem for a system of differential-algebraic equations by some method-of-lines approach. We took the same route in our work and use fourth-order central finite differences to approximate spatial derivatives. In the optimal control formulation we consider only the time-invariant parameters just mentioned as free variables.

In order to evaluate the objective function, the sensitivities of the measured quantity x with respect to the unknown pa-

rameter, $s = (\partial x/\partial D)$, have to be known. For the computation of the gradient of the objective with respect to the parameters p second-order derivatives [here $(\partial^2 x/\partial D \partial p)$] are required. The efficient solution of such optimization problems is still a field of active research (e.g, Bauer et al., 2000). Therefore, we derive the sensitivity equations analytically by differentiation of the model equations. For binary mixtures, the sensitivity equation is given as

$$c_t\left(\frac{\partial s_1}{\partial t} + v_z^* \cdot \frac{\partial s_1}{\partial z}\right) = \frac{\partial}{\partial z}\left(\frac{1}{c_t}\frac{\partial c_t}{\partial D} J_1 - \frac{\partial J_1}{\partial D}\right) - c_t \frac{\partial v_z^*}{\partial D}\frac{\partial x_1}{\partial z} + J_1(V_1 - V_2)\left[c_t \frac{\partial s_1}{\partial z} - c_t^2 (V_1 - V_2) s_1 \frac{\partial x_1}{\partial z}\right], \quad (18)$$

with

$$s_1(z, 0) = 0 \qquad \text{and} \qquad \left.\frac{\partial s_1}{\partial z}\right|_{z = \{0, L\}} 0,$$

where

$$\frac{\partial c_t}{\partial D} = -c_t^2 (V_1 - V_2) s_1 \quad (19)$$

$$\frac{\partial v_z^*}{\partial D} = -(V_1 - V_2)\frac{\partial J_1}{\partial D} \quad (20)$$

$$\frac{\partial J_1}{\partial D} = -c_t\left(\frac{\partial x_1}{\partial z} + D\frac{\partial s_1}{\partial z}\right) - \frac{\partial c_t}{\partial D} D \frac{\partial x_1}{\partial z}. \quad (21)$$

We implemented the model augmented by the sensitivity equation. The optimization problem is then given by

$$\max_{\boldsymbol{p}} \quad F(D, \boldsymbol{p}) \quad (22)$$

s.t. Eqs. 8, 9, 10, 11, 14

Eqs. 18, 19, 20, 21

$$\boldsymbol{p}_l \le \boldsymbol{p} \le \boldsymbol{p}_u.$$

This problem can be solved by standard software for dynamic optimization.

Since the objective function depends on the unknown value of the diffusion coefficient, D, as indicated in Eq. 22, an iterative procedure has to be applied in order to develop an optimal design. Here we have followed the general procedure outlined in Figure 6. Starting from an initial guess for the unknown diffusion coefficient, a first experimental design is found. Here the initial value of the diffusion coefficient is obtained by using the correlation of Siddiqi and Lucas (1986) for the diffusion coefficients at infinite dilution, D_0, and the correlation of Vignes (1966) to interpolate for the mixture composition as recommended by Taylor and Krishna (1993). The thermodynamic factor is calculated using VLE data from Gmehling and Onken (1988). The initial experimental design is then implemented and an experiment is performed. The diffusion coefficient is estimated from the concentration data. If the accuracy of the estimate is insufficient, a new experiment is set up based upon the new value of the diffusion coefficient; otherwise, the diffusion coefficient is found.

The results for the optimal experimental design will be presented for the example system of toluene–cyclohexane. This mixture was chosen because of its ideal behavior for Raman spectroscopy and because density and diffusion data are known from the literature (Sanni et al., 1971). The given data and further density measurements (A. Pfennig, personal communication, 2002) show that the volume of mixing V^E is negligible for this mixture. Therefore, the simpler model (Eqs. 10 and 11) described earlier is sufficient in this case.

The results shown here use a fixed total height of the diffusion cell of $L = 25$ mm. The spatial resolution corresponds to a typical value for the current setup ($\Delta z = 0.025$ mm), and 60

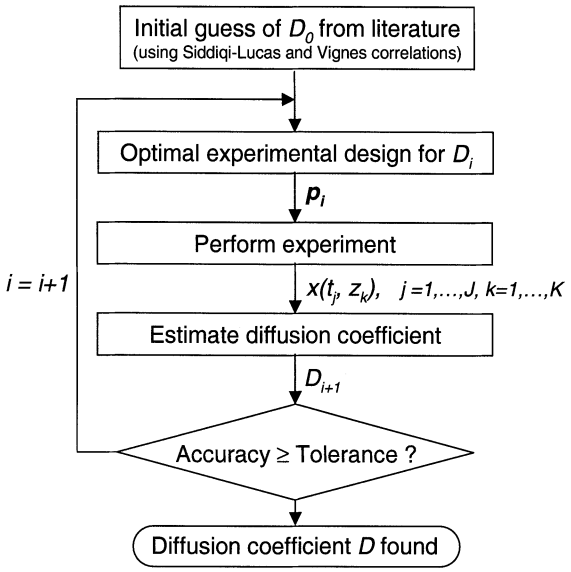

Figure 6. Iterative experimental procedure.

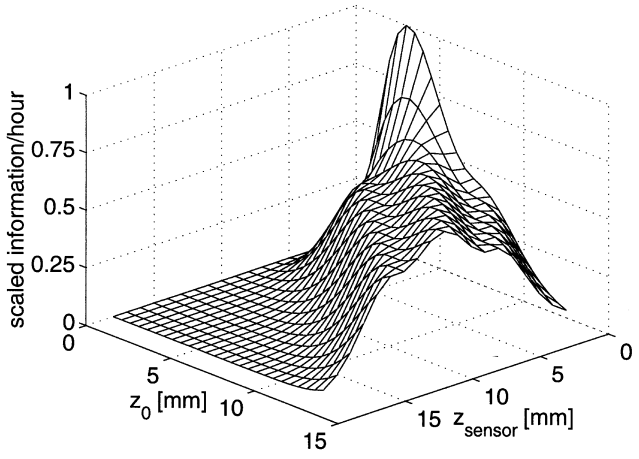

Figure 7. Scaled values for Fisher information measure for $t_{end} = 1$ h.

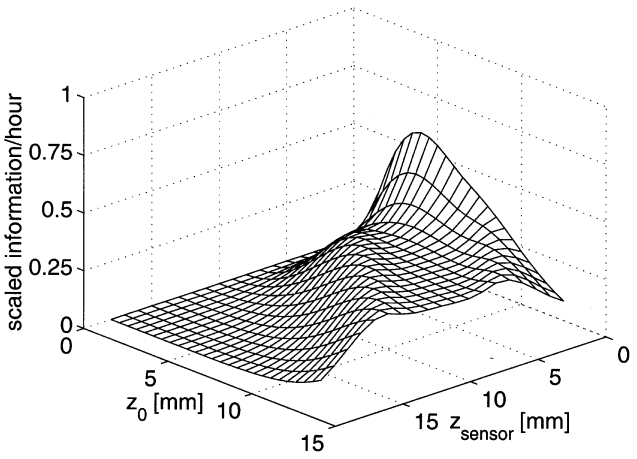

Figure 8. Scaled values for Fisher information measure for $t_{end} = 2$ h.

profiles were obtained over time in each experiment. According to the data from the literature (Sanni et al., 1971), the initial estimate of the diffusion coefficient is fixed at $D_0 = 1.839 \times 10^{-9} \mathrm{m}^2/\mathrm{s}$. Figures 7 and 8 compare the scaled value of the Fisher information measure for different initial setups, measurement positions, and duration of the experiment. It can be clearly seen that it is beneficial to perform the measurements close to the boundary of the system. Furthermore, it is optimal to use small amounts of the heavier phase as the initial condition. This is again due to the fact that the highest sensitivity with respect to the diffusion coefficient is found at the wall. If the lower phase is small, the diffusion front reaches the wall early.

Our experience indicates that the experimental design is rather insensitive to the value of the diffusion coefficient. This is in accordance with the analysis of Emery and Nenarokomov (1998), who observed low nonlinearity of the heat equation with respect to the transfer coefficient. For all measured values of the diffusion coefficient D, it was found to be optimal to position the measurement zone at the boundary. Only the optimal amount of initial substance is dependent on the value of the diffusion coefficient. Furthermore, it is advantageous to perform repeated short experiments instead of just a few longer runs.

The benefit of the use of optimal experimental design techniques will be demonstrated by comparison with two other designs.

- First, we consider the setup most commonly used today to obtain precise measurements of diffusion coefficients by interferometry. Here, the diffusion experiment is performed in a similar diffusion cell, but free boundary conditions are required. The measurement then takes place around the position of the initial sharp interface.
- A second design is the "intuitive design," which is to fill the diffusion cell equally with both mixtures and to observe the zone around the initial boundary.

Table 1 compares the variance of the diffusion coefficient obtained by these two designs with the optimum found. The precision of the measured diffusion coefficient can be substantially improved by careful selection of the free variables

Table 1. Comparison of Diffusion-Coefficient Variance for Different Experimental Design

Design	Free Diffusion	Intuitive Design	Optimal Design
Scaled variance ($\sigma_D^2/\sigma_{D,\mathrm{opt}}^2$)	3.03	3.31	1.0

of the measurement procedure. The analysis shows that the variance of the estimated diffusion coefficient can be reduced by a factor of 3.0 to 3.3 by using the optimal experimental setup compared to the design used in practice today and the intuitive design.

Model-Based Estimation of Diffusion Coefficients

In order to infer the coefficient from the concentration measurements, a nonlinear parameter estimation problem with a system of partial and algebraic equations as constraints has to be solved. This formulation is more flexible than the methods depending on an analytical solution for the diffusion coefficient. Our goal is to minimize the experimental effort by exploiting the possibilities of the optimization approach. In most diffusion measurement techniques depending on the stable layering of two liquids, a sharp interface between the two mixtures is used as an initial condition. This condition is usually obtained by feeding the two phases from both ends of the diffusion cell and withdrawing of the mixture at the position of the interface (Dunlop et al., 1972).

In contrast, our method does not require a sharp phase interface. Instead, the initial profile itself is estimated together with the diffusion coefficient. Due to this procedure the preparation time for each experiment is negligible.

In our approach the first measurement corresponds to time $t = 0$. The profile is smoothed by a smoothing spline routine (Reinsch, 1967). In order to compensate for nonidealities from the experimental procedure, a potential correction of this profile is introduced by adding a spline function to the initial profile. The parameters $\boldsymbol{\Theta}$ of this correction spline are additional free variables of the optimization problem. The initial condition $x_0(z)$ is therefore estimated from

$$x_0(z) = x_{\mathrm{spline}}(\boldsymbol{\Theta}, z) + x_{\mathrm{smooth}}(x_{0,\mathrm{measured}}, z). \quad (23)$$

Assuming the measurement errors to be additional and normally distributed, the maximum likelihood formulation reduces to standard weighted least squares, which can be formulated as

$$\min_{\boldsymbol{\Theta}, D} \sum_{j=1}^{J} \sum_{k=1}^{K} w_{jk} \left[x(t_j, z_k) - f(t_j, z_k, D, \boldsymbol{\Theta}, \boldsymbol{p}) \right]^2, \quad (24)$$

constrained by the model equations and bounds. This problem can be solved with standard software for parameter estimation in dynamical systems.

The effect of simultaneous estimation of the diffusion coefficient and initial condition was tested in numerical investigations. In order to illustrate the effect, a simpler parameterization of the initial condition will be analyzed. Investigators

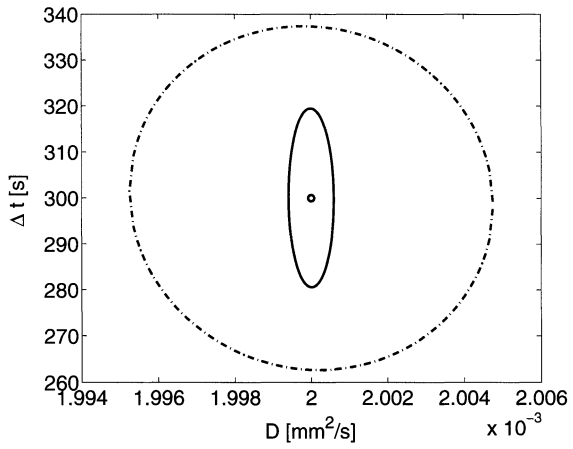

Figure 9. Confidence ellipsoid for two measurements (dash-dotted line) and 60 measurements (solid line).

(see Dunlop et al., 1972) usually compensate for an imperfect interface by introducing an offset time span, Δt. The finite width of the initial boundary corresponds here to the effective time, Δt, it would have taken for an infinitely sharp boundary to diffuse to that width (Miller et al., 1993). Based on simulated data we calculated the confidence ellipsoids for the parameters. Figure 9 shows the results for the case of just two profiles and a complete set of profiles.

It can be seen that the two variables are not correlated even if only two profiles are considered. The correlation coefficient is $R_{12} = R_{21} = -0.0179$. This study indicates that no information concerning the desired diffusion coefficient is lost by the additional estimation of the initial condition.

The simple parameterization with an offset of Δt is not able to properly capture the initial profile obtained by our fast experimental procedure. Therefore, we introduced the spline correction as explained earlier. The analysis of the spline showed similar results. There always is a very small correlation between the diffusion coefficient and the spline parameters. The number of spline parameters was chosen to minimize the correlation between them. Based upon this analysis, the described method is applied to the real data obtained by Raman spectroscopy.

Experimental Results

Piecewise constant estimation of diffusion coefficients

For validation of the new measurement technique we have studied the thermodynamically nearly ideal binary mixture of toluene (1)–cylohexane (2) at a temperature of $T = 294.15$ K (21°C). Each of the four experiments took about 1.5 h, during which we recorded 60 concentration profiles. The spatial resolution, Δz, was calculated as 0.0220 mm (MF 0.9146).

The estimation procedure was carried out as just described. A plot of the residuals over time showed substantial lack-of-fit for the model. The analysis showed that the exact position of the lower boundary is crucial for the correct estimation. Therefore, an additional parameter, Δz_0, was introduced in the estimation problem in order to compensate for errors in the positioning of the diffusion cell relative to the optical axis. Because of the high flexibility of the model-based estimation procedure, the inclusion of a further parameter is straightforward.

The results are presented in Table 2. It includes the initial concentrations of the two phases, x_I, x_{II}, the calculated mutual diffusion coefficients, D, and associated uncertainties.

The quality of the final estimation is assessed by a comparison of the residual sum of squares (RSS) with the value obtained by fitting a smoothing spline to the data. Since the smoothing spline simply removes the noise without considering any physical dependencies, its residual can be taken as a lower bound for any model based on first principles. It can be seen from Table 2 that the model fits the data very accurately. The residual sum of squares is only 1.6 to 3.8 times larger than the value obtained by smoothing. This value is very small, considering that there are still systematic measurement errors that cannot be estimated.

It should be noted that correlation between the introduced coordinate shift, Δz_0, and the diffusion coefficient, D, is substantial. Values for the correlation coefficient, $R_{12} = R_{21}$, range from 0.75 to 0.84. The exact measurement of the boundary position will therefore be included in further investigations.

Figure 10 compares the measured values for the diffusion coefficient with estimates from the literature. The figure

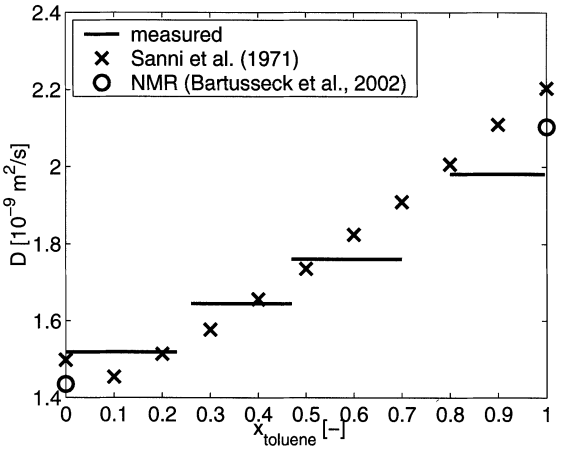

Figure 10. Estimated diffusion coefficient vs. literature data and NMR measurements.

Table 2. Estimated Diffusion Coefficients and Precision for the System Toluene–Cyclohexane at 21°C

Conc. Range $x_I - x_{II}$	D [10^{-9}m²/s]	Δz_0 [mm]	RSS	RSS (Spline)
0.00–0.23	1.5179 ± 0.0022	0.1211 ± 0.0025	6.86×10^{-3}	1.82×10^{-3}
0.26–0.47	1.6445 ± 0.0031	0.3811 ± 0.0039	10.6×10^{-3}	2.91×10^{-3}
0.47–0.70	1.7604 ± 0.0029	0.3134 ± 0.0034	19.2×10^{-3}	11.8×10^{-3}
0.80–1.00	1.9818 ± 0.0037	0.1890 ± 0.0034	7.57×10^{-3}	3.88×10^{-3}

shows the estimated piecewise constant coefficients, the values from Sanni et al. (1971), and NMR measurements of tracer-diffusion coefficients (I. Bartusseck, S. Stapf, and B. Blümich, personal communication, 2002). The tracer-diffusion coefficients, D^*, of cyclohexane and toluene correspond to the values of the Fick diffusion coefficients, $D(x_{\text{toluene}}=1)$ and $D(x_{\text{toluene}}=0)$, at infinite dilution (Cussler, 1976). The values given are extrapolated from a fit to several tracer diffusion experiments. Their relative error is given by $\pm 3\%$. The temperature correction of the values was performed using Tyn's correlation (Reid et al., 1987). Figure 10 shows that the diffusion coefficients measured by the new technique are in accordance with the other results. There is a difference in the region of high toluene concentration. But it should be noted that in the work of Sanni et al. (1971) the values at infinite dilution were obtained by extrapolation of a fitted polynomial. The NMR data points suggest that the true value is lower than the measurements by Sanni et al. (1971). A rigorous comparison will be performed with the temperature-controlled cell.

Direct estimation of concentration dependence

The established methods for the measurement of diffusion coefficients require several point measurements of the diffusion coefficient to be made. The values are then interpolated to estimate the concentration dependence over the whole concentration range. In contrast, our model-based approach offers the possibility of estimating the concentration dependence of the diffusion coefficient directly. For the toluene–cyclohexane system, the concentration dependence of the Fick diffusion coefficient can be approximated by a low-order polynomial with good accuracy (Sanni et al., 1971). Therefore, we propose two candidate models for the diffusion coefficient

$$D_L = D_{CT}x_T + D_{TC}(1-x_T), \tag{25}$$

$$D_Q = D_{CT}x_T + D_{TC}(1-x_T) + D_{\text{quad}}(x_T-0.5)^2. \tag{26}$$

These functions replace the constant coefficient D in Eq. 14. Since the developed model is able to describe the whole concentration range, we can use the data from all runs simultaneously to estimate the unknown coefficients in the model (Eqs. 25, 26). The offset Δz_0 and the correction spline values were taken from the fits shown before in order to reduce correlation. The results are shown in Figure 11.

The diffusion coefficient was estimated as

$$D_L = \left[2.028x_T + 1.433\,(1+x_T)\right]\times 10^{-9}\ \text{m}^2/\text{s}, \tag{27}$$

$$D_Q = \left[2.028x_T + 1.394(1-x_T) + 0.288(x_T-0.5)^2\right] \times 10^{-9}\ \text{m}^2/\text{s}. \tag{28}$$

The residual sum of squares is only 2.5 times larger than the value obtained by spline smoothing. This shows a very good accuracy for the fit. On the other hand, the residual value for the quadratic model is only 10.7% smaller than for the linear case. This suggests that the additional parameter in the model might be statistically ill-determined.

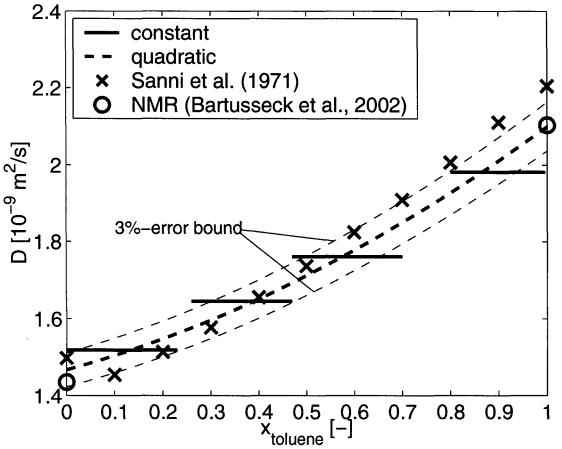

Figure 11. Estimated concentration dependence of diffusion coefficient.

The results show that the new experimental technique allows the direct estimation of the concentration dependence with good accuracy. This makes the measurement of single points in a large number of experiments and the interpolation by a polynomial unnecessary. In principle, it should be possible to obtain all information from a single experiment.

Conclusions

The development of a suitable model for diffusive mass transfer in liquid multicomponent mixtures is not possible today due to the limited experimental data available. In this work we presented a new measurement technique combining Raman spectroscopy and model-based methods for the experimental analysis. The aim of the development is the measurement of diffusion in multicomponent reactive mixtures.

The advantage of the use of spectroscopic methods is their general ability to directly determine the mole fractions of all components in multicomponent mixtures. In this work Raman spectroscopy has been applied for the first time to the high-resolution measurement of concentrations in binary liquid mixtures. The experimental setup has been optimized using model-based techniques. This led to the use of restricted diffusion experiments improving the measurement precision of the diffusion coefficient over conventional designs by a factor of 3.0. The duration of the experiment could be reduced by selecting optimal experimental times. Furthermore, the use of model-based techniques does not require a step profile for the initial concentration. This reduces the experimental preparation time substantially. In the model-based approach it is also possible to determine the diffusion coefficient with its concentration dependence directly from the experimental data. These results from the application of these model-based techniques can be used as well to enhance other diffusion measurement techniques. The novel method has been illustrated with the toluene–cyclohexane binary system.

In the future, the methodology presented in this work will be applied to multicomponent mixtures where the main benefit of the new measurement techniques is expected. For the

concentration determination with Raman spectroscopy the components must be nonfluorescent and Raman-active. This is in general a minor limitation, but lower precision is expected for mixtures of one atomic species, for example, salt mixtures of NaCl and $MgCl_2$. The combination of modern high-resolution spectroscopic measurement techniques and model-based experimental analysis methods is considered to be the adequate basis for the development of suitable models describing the diffusive mass transport in concentrated liquid mixtures.

Acknowledgments

The authors gratefully acknowledge the financial support of the Deutsche Forschungsgemeinschaft (DFG) within the Collaborative Research Center (SFB) 540 "Model-Based Experimental Analysis of Kinetic Phenomena in Fluid Multi-Phase Reactive Systems." They also thank A. Pfennig (Lehrstuhl für Thermische Verfahrenstechnik, RWTH Aachen) and I. Bartusseck, S. Stapf, and B. Blümich (Lehrstuhl für Makromolekulare Chemie, RWTH Aachen) for the additional measurement of material properties.

Notation

A = integral intensity, W/cm·sr
c = concentration, mol/m^3
d = thickness of irradiated sample, m
D = Fick diffusion coefficient, m/s
$Đ$ = Maxwell–Stefan diffusion coefficient, m^2/s
F = Fisher information matrix
I = intensity of radiation, W/cm^2·sr
J = diffusion molar flow, mol/m^2·s
k = calibration factor Raman assembly
L = height of diffusion cell, m
MF = optical magnification factor
N = number of experiments
n_c = number of components in a mixture
$\boldsymbol{p}$ = free variables in experimental setup
r = radius of laser beam, m
R = correlation matrix
s = Raman scattering coefficient, cm^{-1}·sr^{-1}
s = sensitivity of x with respect to D, s/m^2
t = time, s
T = temperature, K
u^V = convective bulk velocity in volume-average reference frame, m/s
v_z^* = convective bulk velocity in molar-average reference frame, m/s
V = specific molar volume, m^3/mol
w = weight in least-squares objective
x = molar fraction
z = spatial direction

Greek letters

γ_i = activity coefficient of component i
ϵ_O = total optical efficiency
$\boldsymbol{\Theta}$ = spline parameters
ν = frequency, m
Φ = radiant power, W
$\Delta\tau$ = time of exposure

Subscripts and superscripts

0 = pure component
C = cyclohexane
i, j, k, l = components i, j, k, and l
L = linear
t = total mixture
Q = quadratic
T = toluene
E = excess
V = volume-fixed reference frame

Literature Cited

Alifanov, O. M., *Inverse Heat Transfer Problems*, Springer-Verlag, Berlin (1994).
Bard, Y., *Nonlinear Parameter Estimation*, Academic Press, New York (1974).
Bauer, I., H. G. Bock, S. Körkel, and J. P. Schlöder, "Numerical Methods for Optimum Experimental Design in DAE Systems," *J. Comput. Appl. Math.*, **120**, 1 (2000).
Bausa, J., and W. Marquardt, "Detailed Modeling of Stationary and Transient Mass Transfer Across Pervaporation Membranes," *AIChE J.*, **47**, 1318 (2001).
Crank, J., *The Mathematics of Diffusion*, Clarendon, Oxford (1975).
Cussler, E. L., *Multicomponent Diffusion*, Elsevier, Amsterdam (1976).
Dieses, A. E., J. P. Schlöder, H. G. Bock, and O. Richter, "Optimal Experimental Design for Parameter Estimation in Column Outflow Experiments," *Tech. Rep. 2000-17, SFB 359: Reaktive Strömungen, Diffusion und Transport*, IWR Heidelberg. http://www.iwr.uni-heidelberg.de/sfb359/Preprints2000.html (2000).
Dunlop, P. J., B. J. Steel, and J. E. Lane, "Experimental Methods for Studying Diffusion in Liquids, Gases and Solids," *Physical Methods of Chemistry*, Vol. I, A. Weissberger and B. W. Rossiter, eds., Wiley, New York, p. 205 (1972).
Emery, A. F., and A. V. Nenarokomov, "Optimal Experimental Design," *Meas. Sci. Technol.*, **9**, 864 (1998).
Gmehling, J., and U. Onken, *Vapor Liquid Data Collection*, DECHEMA, Frankfurt (1988).
gPROMS Technical Document, *The gPROMS User's Guide*, Process Systems Enterprise Ltd., London (2001).
Grünefeld, G., M. Schuette, and P. Andresen, "Simultaneous Multiple-Line Raman/Rayleigh/LIF Measurements in Combustion," *Appl. Phys. B*, **70**, 309 (2000).
Koss, H.-J., M. Behmann, V. Göke, R. Heggen, and K. Lucas, "Auswerteverfahren zur Analyse von Spektren mit stark überlagerten Linien," *Internal Tech. Rep. SFB 540*, RWTH Aachen (2001).
Kyritsis, D. C., P. G. Felton, Y. Huang, and F. V. Bracco, "Quantitative Two-Dimensional Instantaneous Raman Concentration in a Laminar Methane Jet," *Appl. Opt.*, **39**, 6771 (2000).
Leaist, D. G., "Determination of Ternary Diffusion Coefficients by the Taylor Dispersion Method," *J. Phys. Chem.*, **94**, 5180 (1990).
Mewes, B., G. Bauer, and D. Brueggemann, "Fuel Vapour Measurements by Linear Raman Spectroscopy Using Spectral Discrimination from Droplet Interferences," *Appl. Opt.*, **38**, 1040 (1999).
Miller, D. G., J. G. Albright, R. Mathew, C. M. Lee, J. A. Rard, and L. B. Eppstein, "Isothermal Diffusion-Coefficients of NaCl-$MgCl_2$-H_2O at 25-Degrees-C. 5. Solute Concentration Ratio of 1/1 and Some Rayleigh Results," *J. Phys. Chem.*, **97**, 3885 (1993).
Rabenstein, F., and A. Leipertz, "One-Dimensional, Time-Resolved Raman Measurements in a Sooting Flame with 355-nm Excitation," *Appl. Opt.*, **37**, 4937 (1998).
Rai, G. P., and H. T. Cullinan, "Diffusion Coefficients of Quaternary Liquid System Acetone–Benzene–Carbon Tetrachloride–nHexan at 25 C," *J. Chem. Eng. Data*, **18**, 213 (1973).
Reid, R. C., J. M. Prausnitz, and B. E. Poling, *The Properties of Gases and Liquids*, McGraw-Hill, New York (1987).
Reinsch, C. H., "Smoothing by Spline Functions," *Numer. Math.*, **10**, 177 (1967).
Sanni, S. A., C. J. D. Fell, and H. P. Hutchison, "Diffusion Coefficients and Densities for Binary Organic Liquid Mixtures," *J. Chem. Eng. Data*, **16**(4), 424 (1971).
Schrader, B., *Infrared and Raman Spectroscopy*, VCH, Weinheim, Germany (1995).
Siddiqi, M. A., and K. Lucas, "Correlations for Prediction of Diffusion in Liquids," *Can. J. Chem. Eng.*, **64**, 839 (1986).
Taktak, R., J. V. Beck, and E. P. Scott, "Optimal Experimental Design for Estimating Thermal Properties of Composite Materials," *Int. J. Heat Mass Transfer*, **36**(12), 2977 (1993).

Taylor, R., and R. Krishna, *Multicomponent Mass Transfer*, John Wiley, New York (1993).
Unger, J., A. Kröner, and W. Marquardt, "Structural-Analysis of Differential-Algebraic Equation Systems—Theory and Applications," *Comput. Chem. Eng.*, **19**(8), 867 (1995).
Vande Wouwer, A., N. Point, S. Porteman, and M. Remy, "An Approach to the Selection of Optimal Sensor Locations in Distributed Parameter Systems," *J. Process Control*, **10**(4), 291 (2000).
Vignes, A., "Diffusion in Binary Liquids," *Ind. Eng. Chem. Fundam.*, **5**, 189 (1966).
Walter, E., and L. Pronzato, "Qualitative and Quantitative Experiment Design for Phenomenological Models—A Survey," *Automatica*, **26**(2), 195 (1990).

Manuscript received Mar. 15, 2002, and revision received July 18, 2002.